Bioconjugate Chemistry

Article

pubs.acs.org/bc

Efficacy, but Not Antibody Titer or Affinity, of a Heroin Hapten Conjugate Vaccine Correlates with Increasing Hapten Densities on Tetanus Toxoid, but Not on CRM_{197} Carriers

Rashmi Jalah,[†,‡] Oscar B. Torres,[†,‡] Alexander V. Mayorov,[†,‡] Fuying Li,[§,¶] Joshua F. G. Antoline,[§,¶] Arthur E. Jacobson,[§,¶] Kenner C. Rice,[§,¶] Jeffrey R. Deschamps,[∥] Zoltan Beck,[†,‡] Carl R. Alving,[†] and Gary R. Matyas*[,†]

[†]Laboratory of Adjuvant and Antigen Research, US Military HIV Research Program, Walter Reed Army Institute of Research, 503 Robert Grant Avenue, Silver Spring, Maryland 20910, United States

[‡]U.S. Military HIV Research Program, Henry M. Jackson Foundation for the Advancement of Military Medicine, 6720A Rockledge Drive, Bethesda, Maryland 20817, United States

[§]Drug Design and Synthesis Section, Molecular Targets and Medications Discovery Branch, National Institute on Drug Abuse, National Institutes of Health, Department of Health and Human Services, 9800 Medical Drive, Bethesda, Maryland 20892, United States

[¶]National Institute on Alcohol Abuse and Alcoholism, National Institutes of Health, 9800 Medical Drive, Bethesda, Maryland 20892, United States

[∥]Center for Biomolecular Science and Engineering, Naval Research Laboratory, 4555 Overlook Avenue SW, Washington, DC 20375, United States

Supporting Information

ABSTRACT: Vaccines against drugs of abuse have induced antibodies in animals that blocked the biological effects of the drug by sequestering the drug in the blood and preventing it from crossing the blood-brain barrier. Drugs of abuse are too small to induce antibodies and, therefore, require conjugation of drug hapten analogs to a carrier protein. The efficacy of these conjugate vaccines depends on several factors including hapten design, coupling strategy, hapten density, carrier protein selection, and vaccine adjuvant. Previously, we have shown that **1** (MorHap), a heroin/morphine hapten, conjugated to tetanus toxoid (TT) and mixed with liposomes containing monophosphoryl lipid A [L(MPLA)] as adjuvant, partially blocked the antinociceptive effects of heroin in mice. Herein, we extended those findings, demonstrating greatly improved vaccine induced antinociceptive effects up to 3% mean maximal potential effect (%MPE). This was obtained by evaluating the effects of vaccine efficacy of hapten **1** vaccine conjugates with varying hapten densities using two different commonly used carrier proteins, TT and cross-reactive material 197 (CRM_{197}). Immunization of mice with these conjugates mixed with L(MPLA) induced very high anti-**1** IgG peak levels of 400−1500 μg/mL that bound to both heroin and its metabolites, 6-acetylmorphine and morphine. Except for the lowest hapten density for each carrier, the antibody titers and affinity were independent of hapten density. The TT carrier based vaccines induced long-lived inhibition of heroin-induced antinociception that correlated with increasing hapten density. The best formulation contained TT with the highest hapten density of ≥30 haptens/TT molecule and induced %MPE of approximately 3% after heroin challenge. In contrast, the best formulation using CRM_{197} was with intermediate **1** densities (10−15 haptens/CRM_{197} molecule), but the % MPE was approximately 13%. In addition, the chemical synthesis of **1**, the optimization of the conjugation method, and the methods for the accurate quantification of hapten density are described.

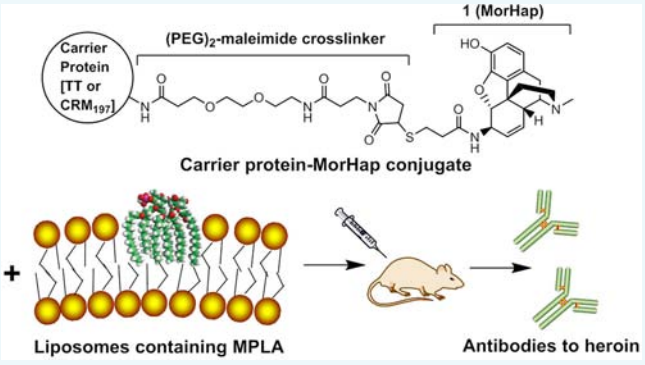

INTRODUCTION

Development of conjugate vaccines including those against drug abuse present the difficult challenge of immunization with small nonimmunogenic haptenic molecules that are unable to induce antibodies on their own following injection or inhalation. Candidate vaccines of this type utilize structurally similar, synthetic surrogate drug analog haptens that are covalently conjugated to protein molecules (carriers) as

Received: February 9, 2015
Revised: April 9, 2015
Published: May 13, 2015

DOI: 10.1021/acs.bioconjchem.5b00085
Bioconjugate Chem. 2015, 26, 1041−1053

Scheme 1. Synthesis of the Heroin Hapten 1

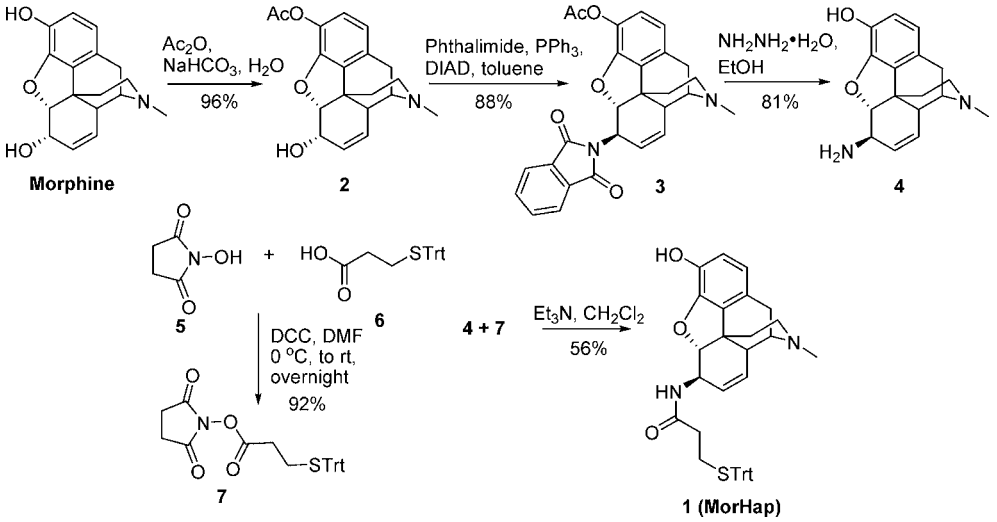

immunogens in order to produce antibodies to the hapten.[1−7] The immunogenicity and efficacy of such a candidate heroin hapten-carrier conjugate vaccine will depend on many factors, including hapten design,[8−10] choice of the carrier protein,[1,11−13] carrier coupling strategy,[14,15] hapten density (the hapten:carrier molar ratio),[10,16,17] and an effective adjuvant formulation that is suitable for human use.[1]

We have now established unique optimized and reproducible methods to prepare and characterize hapten conjugates with maximal hapten densities, in high protein yields, for inducing maximal immunogenicity and inhibition of heroin antinociception. The maximal densities have not hitherto been determined. We have also ascertained the correct hapten densities for **1** (MorHap), a heroin/morphine hapten conjugated to two different, widely used carrier proteins, TT[18,19] and cross-reactive material 197 (CRM_{197}, a nontoxic mutant of diphtheria toxin),[20,21] and in so doing enable the technique for other carrier proteins if needed in the future. This work established that TT-**1** vaccine formulations with liposomes containing monophosphoryl lipid A [L(MPLA)] as adjuvant induced higher and more durable inhibition of heroin-induced antinociception than CRM_{197}-**1** vaccine conjugates with L(MPLA). We have noted that that there is an optimal hapten density unique to TT and CRM_{197} for inducing maximal inhibition of heroin antinociception. For TT, higher hapten densities gave superior vaccine responses, whereas for CRM_{197}, intermediate hapten densities were optimal. Increasing hapten densities correlated with protection from heroin challenge for TT-**1** conjugates, but not for CRM_{197}-**1** conjugates. We further noted that antibody titer and affinity were relatively independent of hapten density and carrier. These studies have greatly improved the efficacy of our previously described TT-**1** vaccine (33 ± 11.5% to 3 ± 1.7% MPE), which had a suboptimal hapten density and conjugation strategy.[8]

RESULTS

Synthesis of Heroin Hapten 1 (MorHap). The synthesis of **1** (Scheme 1) followed the 6-amination route outlined by Hutchinson[22] and MacDougall[23] and involved 3-monoacetylation of morphine base using a modified Welsh procedure[24] followed by a Mitsunobu phthalimidation and removal of the phthalimide protection. It concluded with carbodiimide/*N*-hydroxysuccinimide-mediated conjugation of the commercially available trityl-protected mercaptopropionic acid (Trt-Mpa) linker. The four-step synthesis from morphine (Scheme 1) was accomplished in 38% overall yield. The structure of the compounds **2**, **3**, **4**, **1**, and **7** was confirmed by their ^{1}H and ^{13}C NMR spectra (Supporting Information Figures S1 to S5). The stereochemistry at C6 was proven through X-ray crystallographic analysis of an intermediate in that synthesis (**3**, Figure 1 and Tables S1 to S6).

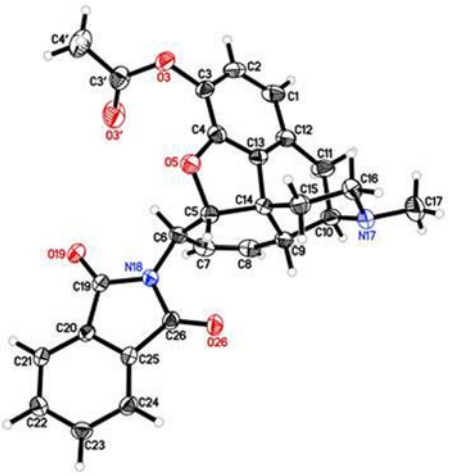

Figure 1. X-ray crystallographic structure of the intermediate **3**.

Conjugation of 1 to TT and CRM_{197} Carrier Proteins. Synthesis of conjugates using optimized methods[25] with 5, 25, 100, 200, 400, and 800 (SM-$(PEG)_2$ linker to carrier protein ratios resulted in a corresponding increase in number of haptens attached of 2, 4, 10, 16, 24, and 30 for TT-**1** (Figure S6) and 1, 3, 10, 15, 19, and 21 for CRM_{197}-**1** (Figure S7) conjugates, respectively, as measured by MALDI-TOF MS. Similar hyperbolic shape quantification curves were observed using two other indirect methods, i.e., the modified Ellman's test which measured the number of maleimides attached after linker addition and the 2,4,6-trinitrobenzenesulfonic acid (TNBS) assay which measured the number of surface amines left unconjugated after hapten addition, indicative of limited

DOI: 10.1021/acs.bioconjchem.5b00085
Bioconjugate Chem. 2015, 26, 1041−1053

attachment sites (Figure 2A,B). Based on the TNBS assay results of the unconjugated protein, the maximum number of

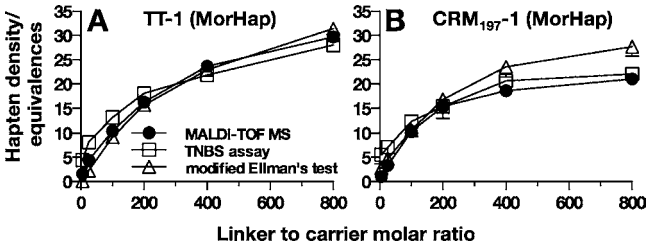

Figure 2. Quantification of number of **1** haptens attached to TT (A) and CRM_{197} (B) carrier proteins upon coupling with increasing molar ratios of SM-$(PEG)_2$ linker to carrier as measured by three different methods. Mean ± SEM from three independent experiments done in triplicates are shown.

amines that were accessible for the attachment of haptens to TT was 27−32 and to CRM_{197} was 21−23. Following hapten attachment, the three methods yielded similar results (Figure 2). MALDI-TOF MS was comparatively superior to the other two chemical strategies as it used smaller amounts of sample and had an easier and faster experimental setup. As determined by the modified Ellman's test, there were no free maleimides on the final conjugates, which confirmed that all the attached linker-maleimides were bound by the hapten.

As determined by BCA, the protein yield of the sterile filtered TT-**1** conjugates was 85−100% (Figure 3, black line)

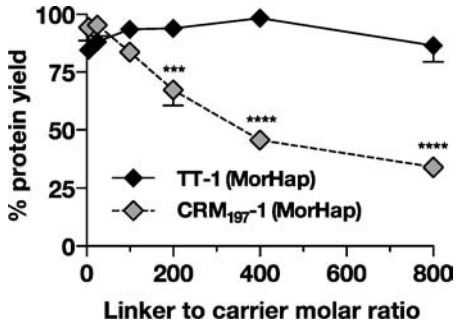

Figure 3. Effect of increasing molar ratios of SM-$(PEG)_2$ linker to carrier protein on the net protein yield of TT-**1** and CRM_{197}-**1** conjugates after conjugation. Mean ± SEM from three independent experiments are shown. The asterisks indicate the linker ratios that resulted in significant decrease in protein yields as compared to the lowest linker ratio (5) (***, $p < 0.001$; ****, $p < 0.0001$) using two-way ANOVA; Dunnett's multiple comparisons test.

for all the linker ratios. For the filtered CRM_{197}-**1** conjugates, the lower linker ratios of 5 and 25 yielded approximately 95% of the starting protein. However, with subsequent increasing linker to carrier ratios of 100, 200, 400, and 800, the protein yield decreased to 84%, 67%, 46%, and 34%, of starting CRM_{197}, respectively (Figure 3, gray symbol). The correct size and integrity of all the filtered conjugates were confirmed by their patterns on nonreducing SDS PAGE and Blue Native PAGE gels (Figure S8) and their SEC-HPLC profiles (Figures S9 and S10). These analyses indicated that none of the conjugates formed any high molecular weight protein aggregates.

Immunogenicity of TT-1 and CRM_{197}-1 Conjugates in Mice. The study design to test the **1**-based vaccines is shown in Figure 4. Three weeks after primary immunization, **1**-specific IgG levels induced by TT-**1** conjugates (Figure 5A) were greater than those induced by CRM_{197}-**1** conjugates (Figure 5B). However, after two injections (week 6) most of the mice had approximately similar IgG levels (0.4−1.5 mg/mL) regardless of the carrier or hapten density used to immunize the animals. Despite some decline during the 5 week period from week 9 to week 14, high levels of IgG antibodies ranging from 0.1 to 0.6 mg/mL were maintained. There was no significant difference between the antibody levels induced by groups having different hapten densities, except that the lowest hapten density group (linker/carrier ratio of 5) for both vaccines gave significantly lower anti-**1** antibodies than the other groups at week 3 ($p = 0.0083$), week 9 ($p = 0.0395$), and week 14 ($p = 0.0016$) for the TT conjugates and at week 9 ($p = 0.0022$) for the CRM_{197} conjugates.

Anti-**1**-specific antibodies (Figure 6, black bars) induced by both carriers at week 9 remained high with increased hapten/carrier ratios, but antibodies specific to the TT (Figure 6A, gray bars) and CRM_{197} (Figure 6B, clear bars) carriers declined with increasing hapten density. The decline in TT responses upon conjugation was less pronounced, and only the highest hapten density group (linker ratio of 800) showed a significant decline up to ∼30-fold ($p < 0.01$). In contrast, the effect of **1** addition on CRM_{197} on the diminution of the anti-CRM_{197} antibody responses was more pronounced with the higher hapten densities [linker ratios of 200 ($p < 0.01$), 400 ($p < 0.05$), and 800 ($p < 0.05$)] showing a significant decline up to ∼90-fold. Also, the TT-specific carrier antibodies were maintained over the 5 week period from week 9 to week 14, whereas the CRM_{197}-specific antibodies significantly declined over time (Figure S11).

Opiate Affinities of Vaccine-Induced Antibodies. As previously reported using competition ELISA,[8] anti-**1** antibodies exhibited higher affinities (lower IC_{50}) to both 6-acetylmorphine and morphine than to heroin ($p < 0.01$) (Table 1). A trend toward possibly higher affinities occurred with higher hapten densities (linker ratios ≥200) for TT-**1** and with lower hapten densities (linker ratios ≤200) for CRM_{197}-**1** conjugates, but this trend was not statistically significant. There was no inhibition of anti-**1** antibodies by codeine (all IC_{50} values were >1000; data not shown).

Blocking of the Effects of Heroin in Mice. Mice injected with TT-**1** showed significant inhibition of heroin-induced antinociception compared to control mice in the tail-flick (Figure 7) and hot plate (Figure 8) tests at week 9 (black bars) and week 15 (gray bars) (tail flick: $p = 0.0003$, week 9; $p = 0.0025$, week 15; and hot plate: $p < 0.0001$, week 9; $p = 0.0024$, week 15). The groups showing better protection not only had lower mean %MPEs, but also showed less variability with almost all mice in the group responding to the vaccine. The highest hapten density group (linker ratio 800, with 30 haptens/TT attached) had the best protection, 3 ± 1.7% MPE on the hot plate assay. TT-**1** hapten density inversely correlated with vaccine efficacy (%MPE) (hot plate weeks 9 and 15: Spearman's $r = -0.89$, $p = 0.03$; tail-flick week 9: $r = -1.0$, $p = 0.003$; tail-flick week 15: not significant $r = -0.43$, $p = 0.42$). In comparison, for CRM_{197}-**1** conjugate vaccines, intermediate hapten densities (linker ratios of 100 and 200 with 10 and 15 haptens/CRM_{197} attached, respectively) gave significantly better inhibition of heroin antinociception that diminished with time (tail flick: $p = 0.0079$, week 9; $p = 0.0295$, week 15; and hot plate: $p = 0.0073$, week 9; $p = 0.1411$, not

DOI: 10.1021/acs.bioconjchem.5b00085
Bioconjugate Chem. 2015, 26, 1041−1053

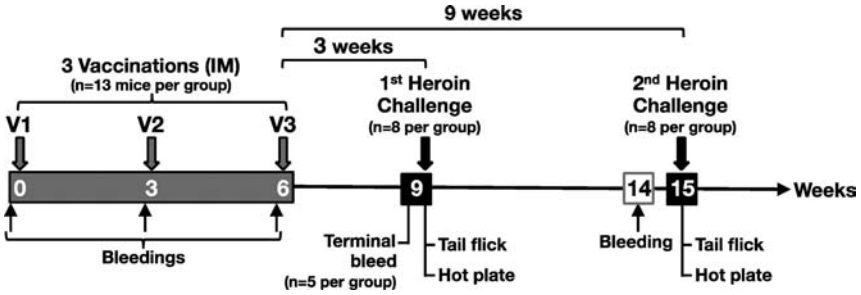

Figure 4. Study design for testing TT-**1** and CRM_{197}-**1** conjugate heroin vaccines in mice. Groups of 13 mice each were IM immunized at weeks 0, 3, and 6 with liposomes containing MPLA as adjuvant. All mice were bled prior to each vaccination. At week 9, 5 mice per group were terminally bled and the remaining 8 mice were challenged with subcutaneous heroin (1 mg/kg). These 8 mice per group were kept longer, bled at week 14 and then re-challenged with heroin at week 15. The vaccine efficacy upon heroin challenge was monitored by the tail flick and hot plate antinociception assays.

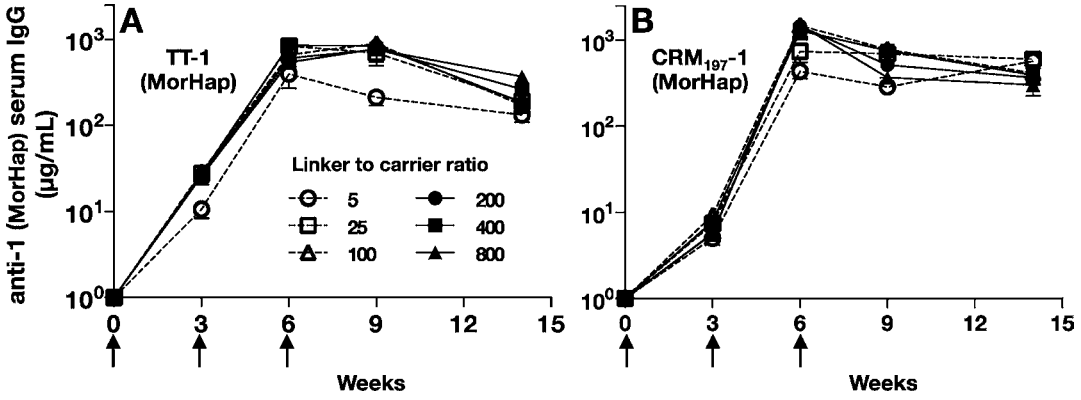

Figure 5. Heroin hapten **1**-specific IgG antibody levels (μg/mL) in sera from mice vaccinated with TT-**1** (A) and CRM_{197}-**1** (B) conjugate vaccines at weeks 0, 3, and 6 (as marked by arrows) and their durability over a period of 2 months after the last vaccination are shown. The groups immunized with conjugates made with varying linker to carrier ratios are marked with different symbols. Values are the mean ± SEM of the 13 mice per group at weeks 0, 3 and 6, the terminally bled 5 mice per group at week 9 and the remaining 8 mice per group at week 14.

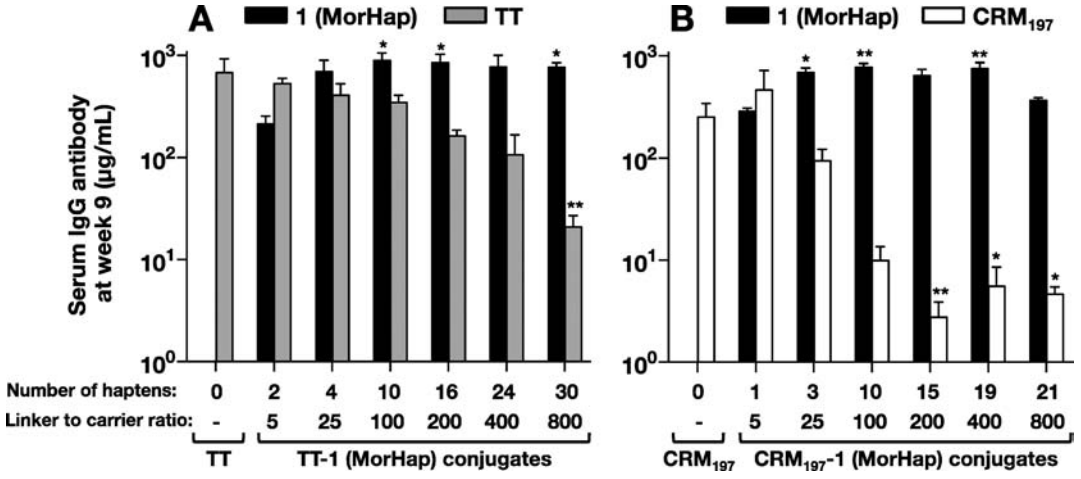

Figure 6. Comparison of anti-**1** (black bars) IgG (μg/mL) to the corresponding anti-TT (A; grey bars) or anti-CRM_{197} (B; clear bars) IgG induced in vaccinated mice at week 9. Bars represent the mean ± SEM for the 4−5 mice per group sacrificed at week 9. The serum IgG levels were quantitated from the corresponding standard curves generated using morphine, TT or CRM_{197} specific mouse monoclonal antibodies in ELISA that was run in triplicates. The number of haptens attached and the corresponding linker to carrier ratios for the different groups are indicated below. Asterisks indicate groups that were significantly different as compared to a control group using one-way ANOVA; Kruskal-Wallis test with Dunn's correction for multiple comparisons (*, $p < 0.05$; **, $p < 0.01$). The control group was the carrier only group for carrier specific antibodies and the lowest hapten density/linker ratio (5) group for **1** specific antibodies.

significant, week 15). As expected, there was no correlation between hapten densities of **1** on CRM_{197} and %MPE. Overall, the inhibition of heroin-induced antinociception elicited by TT-**1** conjugates was higher and more durable than that elicited by the CRM_{197}-**1** conjugates.

DISCUSSION

In this study, the immunogenicity and biological effects of a candidate heroin conjugate vaccine were compared and described using two commonly used carrier proteins, TT and

DOI: 10.1021/acs.bioconjchem.5b00085
Bioconjugate Chem. 2015, 26, 1041−1053

Table 1. Competition of Sera from Mice Immunized with Varying Hapten Densities of Heroin Hapten 1 Conjugated to TT or CRM_{197}

	antibody affinity; IC_{50}[a] (μM) for grouped sera[b]					
	TT-**1** conjugates			CRM_{197}-**1** conjugates		
linker to carrier ratio	heroin	6-acetyl morphine	morphine	heroin	6-acetyl morphine	morphine
5	8553	107	54	2636	37	40
25	3644	53	20	2288	87	21
100	4616	137	72	3143	55	18
200	4565	109	32	1677	105	16
400	3714	72	21	>10000	410	81
800	2522	229	21	6801	249	82

[a]All IC_{50} values (concentration that produced 50% inhibition of maximal binding) were calculated from normalized competition curves using log(inhibitor) vs normalized response-variable slope regression. [b]Data were calculated from the mean of the 4−5 mice grouped by competitive opiate from SI Figure S14.

CRM_{197}, with a varying number of haptens attached. It is generally believed that high titer and affinity antibodies are responsible for substance abuse vaccine efficacy. We hypothesized that increasing hapten density would increase the antibody titer as previously shown for other haptens[26,27] and that this increase in titer would lead to a better vaccine efficacy. We also hypothesized that the carrier protein may also have effects on titer and efficacy. Immunization of mice with **1** coupled to TT or CRM_{197} gave very high and durable IgG anti-**1** levels (0.2−1.5 mg/mL) (Figures 5 and 6). Similar peak antibody levels were obtained using both carriers. However, there were no significant differences in antibody titers to **1** by immunization with higher hapten densities on TT or CRM_{197}, except titers were lower in animals immunized with the lowest hapten density. This is in contrast to the studies reported with other haptens that demonstrated that higher hapten densities induced higher antibody titers.[26,27] The very high antibody level observed to **1** even at low hapten densities may be due to the potency of the L(MPLA) adjuvant used in this study when compared to aluminum based adjuvants used in other studies.[1] Another possible factor in heroin vaccine efficacy may be antibody affinity, but we observed no significant differences in antibody affinities as a function of hapten density or carrier (Table 1). Based on these findings, it is surprising that vaccine efficacy from heroin challenge was correlated with hapten density for the TT-**1** vaccine and was highest at intermediate hapten densities for CRM_{197}. These data imply that there is a yet unidentified factor or factors involved in substance abuse vaccine efficacy.

Similar to our findings, Pravetoni et al.[13] reported that antibody titers did not correlate with vaccine efficacy of an oxycodone hapten vaccine, but reported that hapten-specific B cells correlated with antibody titer. This suggests that the quantity of hapten-specific B cells is not responsible for the increased efficacy of TT-**1** at high hapten densities. One explanation for the increased efficacy observed from the TT-**1** high density conjugates and the intermediate densities of CRM_{197}-**1** is that the antibodies induced were able to bind more than one hapten in the antibody binding site leading to the ability to sequester more heroin molecules. Based on analysis of 111 antigen−antibody X-ray structures, Stave and Lindpaintner[28] reported that the average number of antigen residues that contact the antibody was 18 and that the average antibody residues contacting the antigen was 21. Since heroin (369 Da) is approximately 3 times the mass of an amino acid (110 Da), this suggests that the average antibody binding site could theoretically accommodate up to 6 haptens. The presentation of haptens at high density may result in more than 1 hapten on the same peptide being presented to the B cell receptor, whereas at low hapten densities only 1 hapten is presented. If the antibodies induced by high hapten densities bound multiple heroin molecules, there could be no difference in ELISA titer between antibodies that bind multiple haptens versus a single hapten, since ELISA measures a single interaction of the hapten with antibody.[25]

The development of a vaccine to drugs of abuse has a number of key elements related to the hapten and its conjugation to the carrier, including hapten selection, hapten synthesis yield, reproducible conjugation of the hapten to the carrier, and quantification of the conjugated hapten. The heroin hapten **1**[8,29] used in the study was easily synthesized from morphine in good yields using a four-step scalable procedure with an overall yield of 38% (Scheme 1 and Figure 1). **1** is similar to the C6-linked morphine based haptens previously described.[30−35] **1** contains an amide linker at the C6-position, which is hydrolytically stable in contrast to the ester functional group of the hemisuccinyl linkage.[30−33] An ether linkage to a

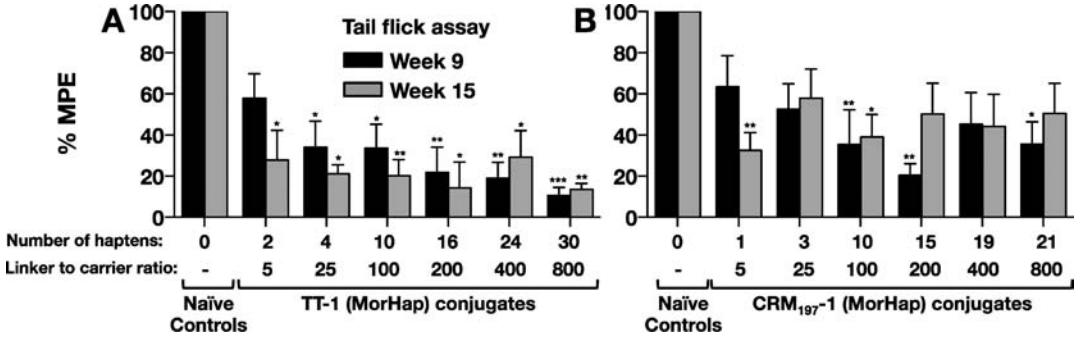

Figure 7. Inhibition of antinociception in the tail flick assay upon heroin challenge elicited by the TT-**1** (A) and CRM_{197}-**1** (B) conjugate heroin vaccines in mice challenged at week 9 (black bars, 3 weeks post last vaccination) and later at week 15 (grey bars, 9 weeks post last vaccination). Bars represent %MPE values ± SEM for the 7−8 mice from each group. The number of haptens attached and the corresponding linker to carrier ratios for the different groups are indicated below. The asterisks indicate groups that were significantly different as compared to the unvaccinated naïve controls (*, $p < 0.05$; **, $p < 0.01$; ***, $p < 0.001$) using one-way ANOVA; Kruskal-Wallis test with Dunn's correction for multiple comparisons.

DOI: 10.1021/acs.bioconjchem.5b00085
Bioconjugate Chem. 2015, 26, 1041−1053

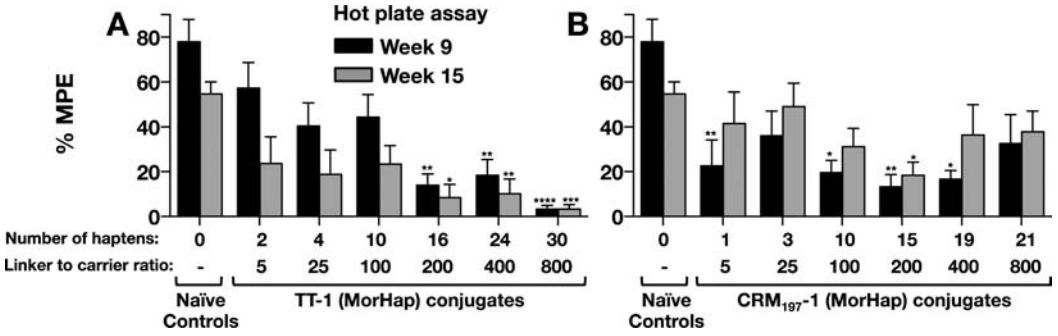

Figure 8. Inhibition of antinociception in the hot plate assay upon heroin challenge elicited by the TT-**1** (A) and CRM_{197}-**1** (B) conjugate heroin vaccines in mice challenged at week 9 (black bars, 3 weeks post last vaccination) and later at week 15 (grey bars, 9 weeks post last vaccination). Bars represent %MPE values ± SEM for the 7−8 mice from each group. The number of haptens attached and the corresponding linker to carrier ratios for the different groups are indicated below. The asterisks indicate groups that were significantly different as compared to the unvaccinated naïve controls (*, $p < 0.05$; **, $p < 0.01$; ***, $p < 0.001$; ****, $p < 0.0001$) using one-way ANOVA; Kruskal-Wallis test with Dunn's correction for multiple comparisons. The control group was common for all panels.

$(Gly)_4$ linker developed by Pentel et al. should have similar chemical stability to that of the C6-amide of **1**,[34,35] but has an overall yield of 20% over five steps in its synthesis. Both the hemisuccinyl and ether linked haptens have a carboxyl terminus, which is used to couple to carrier lysine groups through carbodiimide chemistry, while **1** has a sulfhydryl group for coupling to maleimide linkers. Carbodiimide-mediated coupling is difficult to control resulting in lot-to-lot variability of the number of haptens attached and can lead to intracarrier coupling of Asp and Glu to Lys.[15] In contrast, the maleimide-sulfhydryl coupling used for **1** does not lead to amino acid cross-linking and is easily controlled.[36] This allowed for the investigation of hapten density on the immunogenicity and efficacy of vaccines based on hapten **1**.

In order to conduct the immunological studies with varying hapten densities, we optimized the coupling procedure to both TT and CRM_{197} protein carriers and developed strategies to reproducibly control hapten number based on our previous studies on conjugating **1** to BSA.[25] These optimizations were as follows: (a) purification of the hapten **1** after deprotection to remove the trityl byproducts by a petroleum ether wash to enhance aqueous solubility of the conjugates; (b) use of a desalting column instead of overnight dialysis for removing the excess linker after the linker addition step, which prevented the hydrolysis and loss of maleimide to maleamic acid; and (c) use of overnight dialysis instead of column to remove excess hapten after conjugation in order to prevent losses due to the hydrophobic conjugates sticking or precipitating on the column. This optimization allowed for the reproducible high yield coupling of **1** to TT and CRM_{197}. By altering the linker to carrier ratio, defined hapten densities on both carriers were reproducibly obtained. MALDI-TOF MS was used to quantify the number of haptens conjugated and this was in good agreement with the TNBS and Ellman's assays. As part of the optimization studies, we found that a higher number of the **1** molecules could be attached to TT (27−32) as compared to CRM_{197} (21−23), with minimal loss of protein yield of the conjugates (Figures 2 and 3). TT (152 kDa) has a molecular weight that is 2.6-fold larger than CRM_{197} (58 kDa) and, consequently, has approximately twice the surface area than CRM_{197} (assuming the molecular weight corresponds to the volume of a sphere, thereby allowing for calculation of the radius and then the surface area). In addition, TT is inactivated by formaldehyde resulting in the cross-linking or modification of Lys side chains,[11,19,37] which reduces the number of primary amino groups on its surface available for conjugation. Using the TNBS assay, we measured approximately 30 lysine residues on tetanus toxoid. Untreated tetanus toxin has 106 lysine residues,[18] most of which are on the surface.[19] Consequently, formaldehyde treatment of tetanus toxoid reduced the lysine content by 3.3-fold. Based on the above mathematical analysis, there appears to be a larger spatial distance between the Lys-linked **1** on TT as compared to CRM_{197}, thereby making TT less prone to precipitation upon coupling of similar numbers of haptens. However, some of these surface amines may be clustered together thereby generating antibodies recognizing multiple haptens within a single binding site at high hapten densities. Since formaldehyde treatment leads to side chain modification or cross-linking of varying Lys in different molecules of TT,[19,37] it is not possible to quantitatively identify the exact Lys residues that contain covalently bound hapten in a given molecule.

Although anti-**1** titer was independent of hapten density, the antibody titer to the carriers, TT and CRM_{197}, decreased as a function of increasing hapten density (Figure 6). This is expected as hapten conjugation masks the immunogenic epitopes on the carrier surface. A more pronounced suppression of carrier-specific antibodies with increasing hapten densities was observed for CRM_{197} than TT. The larger carrier protein size to hapten number ratio of TT as compared to CRM_{197}[11] may explain this phenomenon. The TT antibody levels started higher than those of CRM_{197} and were maintained over time. In contrast, anti-CRM_{197} levels were lower at week 9 than anti-TT levels and declined significantly by week 14 reaching undetectable levels for several mice (groups with linker ratios ≥200; Figure S11). This may indicate reduced B cell maturation and memory development with lower T-cell help for CRM_{197}-**1** conjugates as compared to TT-**1** conjugates. This could also explain the lower and less durable efficacy of CRM_{197}-**1** conjugates (Figures 7 and 8).

There are two factors believed to be involved in substance abuse vaccine efficacy: antibody titer and affinity. Since the antibody titers were similar for the different hapten densities, they cannot account for the differences in efficacy. This suggests that differences in affinity must be responsible for the efficacy differences. Examination of the antibody affinities by competition ELISA revealed no significant differences in affinity among the groups. However, anti-**1** antibodies had higher

DOI: 10.1021/acs.bioconjchem.5b00085
Bioconjugate Chem. 2015, 26, 1041−1053

affinities to 6-acetylmorphine and morphine than to heroin (Table 1). Heroin is rapidly metabolized to 6-acetylmorphine within minutes after intravenous injection. Recent studies have shown that 6-acetylmorphine is the predominant form that enters the brain[34] and antibodies blocking it are sufficient to block acute heroin effects.[38] Consequently, the higher affinity of anti-**1** antibodies to 6-acetylmorphine may contribute more to the vaccine efficacy by blocking heroin antinociceptive effects. However, the IC_{50} values were high and most likely are not a reflection of the true dissociation constant of the antisera. As was previously shown, the values obtained by competition ELISA are greatly influenced by the affinity of the antibodies to the hapten used in the assay.[8] If the antibodies have high affinity to the hapten, higher concentrations of competing compound are required to prevent the binding of the antibodies to the hapten coated well. In addition, it is well-known that in competition ELISA, both arms of the antibody are bound to the well and that higher concentrations of competitive drug are required to displace the antibody resulting in higher IC_{50}. In addition, if multiple haptens are able to bind within the antibody binding site, higher concentrations of competitor would be required to prevent the antibody from binding to the ELISA plate. Consequently, the high IC_{50} observed in the present study may represent higher affinity antibodies than reported by others with similar haptens.[33,34,39]

Although the carrier had no effect on anti-**1** antibody titer, the inhibition of antinociception induced by high hapten density groups of TT-**1** vaccines was higher and more durable than that induced by the CRM_{197}-**1** conjugates (Figures 7 and 8), thereby making TT the preferred carrier choice for **1**-based vaccines. Since the same dose of protein (10 μg) was injected for both carrier conjugates, a lower number of total haptens were injected for the larger molecular weight TT-**1** conjugates (154−175 kDa) than the CRM_{197}-**1** conjugates (58−73 kDa). The TT-**1** conjugates were more efficacious than CRM_{197}-**1** conjugates even with a lower number of total molecules/total haptens injected. This further strengthens our conclusion of TT being the preferred carrier of choice for **1**-based vaccines. CRM_{197} conjugates with higher hapten densities failed to give increased protection probably due to the steric hindrance between haptens that blocked their engagement to the B cell receptor as seen before for antibodies to BSA-**1** conjugates.[25] It may also be possible that the CRM_{197} conjugates have lower stability as compared to the TT conjugates that may have been stabilized by the formaldehyde treatment. Although we did not see any protein aggregates or degradation in any of the conjugates on SDS PAGE, Native PAGE, and SEC-HPLC, the bands for CRM_{197}-**1** conjugates did become broader with increasing hapten loading indicating heterogeneous mixtures and possibly lower stability (Figures S8−S10). Alternatively, the CRM_{197} conjugates may be less stable in vivo as compared to the formaldehyde treated TT. Another possibility is that the formaldehyde treatment with TT may lead to multiple haptens presented at the same time. Studies directly comparing the effect of carrier proteins on vaccine immunogenicity, efficacy, and immune interference have varying results in which no overall conclusions can be drawn.[11,40−43] Although TT was a better carrier for our heroin hapten conjugate vaccine, it is not the best vaccine carrier in general for every conjugate vaccine. There are numerous licensed polysaccharide vaccines that use CRM_{197} as a carrier.[20,43,44] In addition, the optimal carrier may be dependent upon the type of antigen coupled (polysaccharides vs small molecules) and the adjuvant and vehicle used in the vaccine formulation. Our results demonstrate the need for head to head comparisons of carriers and that these comparisons are critical for the selection of the best candidates for substance abuse vaccine development.

CONCLUSION

To be successful, a conjugate vaccine for drugs of abuse is required to induce antibodies that are high titer and have long durability and high affinity to the drug and its active metabolites. This is dependent on factors that include hapten design, coupling strategy, hapten density, carrier protein, and adjuvant selection. In this Article, we have demonstrated the following: (1) Immunization with TT-**1** containing 30 heroin hapten **1** molecules per TT molecule gave nearly complete protection of mice from heroin challenge as measured in antinociception assays compared to **1** conjugated to TT and CRM_{197} at other **1** densities. (2) Vaccine efficacy with TT-**1** correlated with hapten **1** density. (3) Immunization with TT-**1** and CRM_{197}-**1** formulated with L(MPLA) induced high titer (up to ∼1.5 mg/mL) and durable IgG to **1** that was relatively independent of carrier, hapten **1** density, and vaccine efficacy. (4) Facile synthesis of **1** produced acceptable yield. (5) Conjugation of **1** at varying hapten densities to TT and CRM_{197} can be reproducibly controlled and measured. Based on these findings, TT-**1** is a viable candidate for a heroin vaccine. It utilizes a hapten that is easily synthesized and hydrolytically stable, a carrier suitable for human use, a potent adjuvant, and induces high titer and long duration antibodies that block the effects of heroin. It can be easily and effectively translated into humans as a synergistic treatment option for heroin addiction.

EXPERIMENTAL PROCEDURES

Synthesis of Heroin Hapten 1. All melting points were determined on a Thomas-Hoover melting-point apparatus and are uncorrected. ^{1}H and APT ^{13}C NMR spectra were recorded on a Bruker DRX-500 spectrometer, and chemical shifts (ppm) were referenced to an internal $CDCl_3$ standard (^{1}H, 7.26 ppm and ^{13}C, 77.0 ppm). High-resolution mass spectra (HRMS) were recorded using electrospray ionization (ESI) or MALDI-TOF techniques. HPLC grade acetonitrile, methanol, and dichloromethane, ACS reagent grade ethanol, and anhydrous (DriSolv) toluene were purchased from EMD Millipore via VWR International (Suwanee, GA). Tritylmercaptopropionic acid (compound **6**, Figure 1, Trt-Mpa) was acquired from Chem-Impex International (Wood Dale, IL). All other chemical reagents and solvents were ACS reagent grade, obtained from Sigma-Aldrich Chem. Co., and were used without further purification. Units for $[\alpha]_D$ values were given in 10^{-1} deg cm^2 g^{-1}. Glassware and solvents were dried by standard methods. Flash chromatography was performed on silica gel 60 (230−400 mesh), and thin layer chromatography (tlc) on glass plates coated with a 0.02, 0.5, or 1.0 mm layer of silica gel 60 F-254. LC-MS analyses were performed on a Waters Acquity UPLC-TQD system (Waters Corp., Milford, MA) at a flow rate of 0.5 mL/min, with detection at 254 nm during a linear gradient of 5−95% acetonitrile/0.09% formic acid over 20 min at 35 °C. Preparative RP-HPLC was performed on a Shimadzu Prominence LC-6AD semipreparative HPLC system using a Vydac 218TP152022 C18 column (Grace Davison Discovery Sciences, Deerfield, IL) at a flow rate of 15 mL/min, with detection at 254 and 280 nm; fractions were analyzed by LC/

DOI: 10.1021/acs.bioconjchem.5b00085
Bioconjugate Chem. 2015, 26, 1041−1053

MS, pooled, and lyophilized to yield the target compounds as amorphous powders.

(4*S*,4a*R*,7*S*,7a*R*,12b*R*)-7-Hydroxy-3-methyl-2,3,4,4a,7,7a-hexahydro-1*H*-4,12-methanobenzofuro-[3,2-*e*]isoquinolin-9-yl acetate (3-acetylmorphine, 2). To a suspension of morphine base (0.3 g, 1.05 mmol) in H_2O (20 mL) was added $NaHCO_3$ (0.26 g, 3.15 mmol) and acetic anhydride (0.21 g, 0.2 mL) and the solution was stirred for 2 h at room temperature. The mixture was extracted with CH_2Cl_2 (5 × 20 mL) and the combined extracts were washed with brine and dried over anhydrous Na_2SO_4. After evaporation of the solvent, **2** was obtained as a yellow foam (0.33 g, 96%). A sample for analysis was purified by flash chromatography ($CHCl_3$–MeOH, 95:5 to 90:10) to give **2** as a white foam (91%). ^{1}H NMR (500 MHz, $CDCl_3$): δ = 6.73 (d, J = 8.5 Hz, 1H), 6.60 (d, J = 8.0 Hz, 1H), 5.74 (d, J = 9.5 Hz, 1H), 5.27 (d, J = 10.0 Hz, 1H), 4.91 (d, J = 7.0 Hz, 1H), 4.16 (s, 1H), 3.38 (s, 1H), 3.05 (d, J = 18.5 Hz, 1H), 2.73 (s, 1H), 2.63 (dd, J = 12.0, 4.0 Hz, 1H), 2.45 (s, 3H), 2.39 (td, J = 12.0, 3.5 Hz, 1H), 2.33 (dd, J = 19.0, 6.5 Hz, 1H), 2.28 (s, 3H), 2.10 (td, J = 12.5, 5.0 Hz, 1H), 1.90 (d, J = 12.0 Hz, 1H). ^{13}C NMR (125 MHz, $CDCl_3$): δ 168.7, 148.8, 134.4, 132.7, 132.3, 131.9, 127.7, 121.2, 120.0, 92.4, 65.9, 59.1, 46.6, 43.1, 42.7, 40.4, 35.2, 20.94, 20.89. MS (ESI): m/z = 328.2 $[M + H]^+$.

HRMS (ESI) m/z: $[M + H]^+$ calcd. for $C_{19}H_{22}NO_4$: 328.1549; found: 328.1558.

(4*S*,4a*R*,7*R*,7a*R*,12b*R*)-7-(1,3-Dioxoisoindolin-2-yl)-3-methyl-2,3,4,4a,7,7a-hexahydro-1*H*-4,12-methanobenzofuro[3,2-*e*]isoquinolin-9-yl acetate (3). To a solution of **2** (100 mg, 0.3 mmol) in toluene (9 mL) was added phthalimide (90 mg, 0.6 mmol) and triphenylphosphine (165 mg, 0.63 mmol) and the solution was stirred at room temperature under argon for 5 min. A solution of diisopropyl azodicarboxylate (DIAD, 121 mg, 0.12 mL, 0.6 mmol) in toluene (1 mL) was added dropwise via syringe, over the course of 4 min. The stirring was continued for 2 h and the solvent was removed under reduced pressure. The yellow syrupy residue was purified by flash chromatography (CH_2Cl_2/acetone, 3:1 to CH_2Cl_2/acetone/CH_3OH, 10:3:1) to give **3** as a white foam (0.12 g, 88%), which was crystallized from EtOH to afford **3** as white crystals (88%); mp 229.3–231.8 °C. $[\alpha]_D^{20}$ −288.8° (c 0.5, $CHCl_3$). ^{1}H NMR (500 MHz, $CDCl_3$): δ = 7.82 (m, 2H), 7.70 (m, 2H), 6.80 (d, J = 8.5 Hz, 1H), 6.64 (d, J = 8.0 Hz, 1H), 5.67 (d, J = 10.0 Hz, 1H), 5.49 (m, 1H), 5.05 (s, 1H), 4.85 (d, J = 3.5 Hz, 1H), 3.44 (s, 1H), 3.33 (t, J = 4.0 Hz, 1H), 3.07 (d, J = 18.5 Hz, 1H), 2.62 (m, 1H), 2.46 (s, 3H), 2.32 (m, 6H), 1.76 (d, J = 9.0 Hz, 1H). ^{13}C NMR (125 MHz, $CDCl_3$): δ 168.4, 167.5 (2), 147.6, 134.2 (2), 132.6, 132.5, 132.0 (2), 131.6, 131.4, 126.6, 123.4 (2), 121.8, 119.5, 91.8, 59.2, 50.9, 47.3, 44.8, 43.1, 40.2, 34.0, 21.0, 20.8; MS (ESI): m/z = 457.2 $[M + H]^+$. HRMS (ESI) m/z: $[M + H]^+$ calcd. for $C_{27}H_{25}N_2O_5$: 457.1763; found: 457.1745. Anal. Calcd for $C_{27}H_{24}N_2O_5$: C, 71.04; H, 5.30; N, 6.14. Found: C, 70.65; H, 5.19; N, 6.16.

X-ray crystal data: The 0.261 × 0.199 × 0.119 mm^3 data crystal was orthorhombic in space group $P2_12_12_1$, with unit cell dimensions a = 12.7710(6), b = 13.1774(7), and c = 13.6891(7) Å. The data was 99.5% complete to 29.19° θ (~0.73 Å) with an average redundancy of 7.74. The final anisotropic full matrix least-squares refinement on F^2 with 96 variables and one constraint converged at R1 = 3.16%, for the observed data and wR2 = 9.65% for all data. The absolute configuration was set based on the known configuration of unvarying chiral centers.

(4*S*,4a*R*,7*R*,7a*R*,12b*R*)-7-Amino-3-methyl-2,3,4,4a,7,7a-hexahydro-1*H*-4,12-methanobenzofuro-[3,2-*e*]isoquinolin-9-ol (4). To a solution of phthalimide **3** (0.12 g, 0.26 mmol) in 95% EtOH was added hydrazine hydrate (0.1 mL) by syringe and the solution was heated at 55 °C for 1.5 h. The solvent was removed in vacuo and the residue was treated with 2 M hydrochloric acid (10 mL) and EtOH (4 mL). The resulting suspension was filtered and the filtrate was basified with ammonia and extracted with $CHCl_3$ (6 × 30 mL). The combined extracts were washed with brine and dried over anhydrous Na_2SO_4. The crude product was purified by flash chromatography ($CHCl_3$/MeOH/NH_4OH, 90:9:1 to 80:18:2) to afford **4** as a white foam (60 mg, 81.0%), which crystallized from Et_2O/isopropanol, 5:1, to give **4** as white crystals (71%); mp 206.5–211.3 °C (lit[45] 214–218 °C). $[\alpha]_D^{20}$ −173.6° (c 0.5, MeOH) (lit[45] −182.5° (c 0.5, MeOH). ^{1}H NMR (500 MHz, $CDCl_3$): δ = 6.59 (d, J = 8.0 Hz, 1H), 6.48 (d, J = 8.0 Hz, 1H), 5.80 (m, 1H), 5.50 (d, J = 10 Hz, 1H), 4.58 (s, 1H), 3.47 (s, 1H), 3.31 (s, 1H), 2.98 (m, 2H), 2.59 (dd, J = 11.5, 3.5 Hz, 1H), 2.40 (s, 3H), 2.30 (m, 2H), 2.03 (td, J = 12.0, 4.5 Hz, 1H), 1.75 (d, J = 11.5 Hz, 1H). ^{13}C NMR (125 MHz, $CDCl_3$): δ = 143.6, 139.7, 131.9, 130.2, 129.2, 125.2, 119.6, 117.6, 95.9, 59.4, 52.5, 47.5, 43.9, 43.0, 39.9, 35.4, 20.4. MS (ESI): m/z = 285.2 $[M + H]^+$. HRMS (ESI) m/z: $[M + H]^+$calcd for $C_{17}H_{21}N_2O_2$ 285.1603; found, 285.1606; Anal. Calcd for $C_{17}H_{20}N_2O_2{\cdot}0.2H_2O$): C, 70.91; H, 7.14; N, 9.73. Found: C, 70.88; H, 7.40; N, 9.53.

2,5-Dioxopyrrolidin-1-yl 3-(tritylthio)propanoate (7). To a stirred solution of 1-hydroxypyrrolidine-2,5-dione (**5**, 305 mg, 2.65 mmol) and 3-(tritylthio)propanoic acid (**6**, 730 mg, 2.09 mmol) in anhydrous DMF (25 mL) at 0 °C was added dicyclohexylcarbodiimide (610 mg, 2.96 mmol) in one portion. The resulting solution was slowly warmed to room temperature and stirred for 24 h. The solution was diluted with Et_2O (100 mL). The solution was washed with H_2O, brine, and dried over $MgSO_4$. After it was concentrated in vacuo, the residue was purified by silica gel chromatography (hexanes/EtOAc, 90:10) to give **7** (860 mg, 92% yield) as a white solid. ^{1}H NMR (500 MHz, $CDCl_3$): δ = 7.45 (d, 6H, J = 7.5 Hz), 7.20–7.33 (m, 9H), 2.78 (s-br, 4H), 2.56 (t, 2H, J = 7.5 Hz), 2.41 (t, 2H, J = 7.5 Hz. ^{13}C NMR (125 MHz, $CDCl_3$): δ = 169.0, 167.2, 144.4, 129.6, 128.2, 126.9, 67.2, 30.6, 26.2, 25.6. HRMS (ESI) m/z: $[M + H]^+$ calcd for $C_{26}H_{23}NO_4SK$ 484.0985; found: 484.1003.

***N*-((4*S*,4a*R*,7*R*,7a*R*,12b*R*)-9-Hydroxy-3-methyl-2,3,4,4a,7,7a-hexahydro-1*H*-4,12-methanobenzofuro-[3,2-*e*]isoquinolin-7-yl)-3-(tritylthio)propanamide (1).** To a solution of **4** (60 mg, 0.21 mmol) in CH_2Cl_2 (5 mL) was added triethylamine (0.06 mL, 0.42 mmol) and activated ester 2,5-dioxopyrrolidin-1-yl 3-(tritylthio)propanoate (**7**, 130 mg, 0.32 mmol), and the solution was stirred for 48 h. Saturated aqueous $NaHCO_3$ was added and the organic layer was separated. The aqueous layer was extracted with CH_2Cl_2 (3 × 30 mL). The combined extracts were washed with brine and dried over anhydrous Na_2SO_4. The crude product was purified by flash chromatography ($CHCl_3$/MeOH/NH_4OH, 95:4.5:0.5 to 80:18:2) to afford the desired hapten **1** as a white powder (72 mg, 55.8%). Starting material **4** (20 mg) was recovered. $[\alpha]_D^{20}$ −134.0° (c 0.5, $CHCl_3$). ^{1}H NMR (500 MHz, $CDCl_3$+CD_3OD): δ = 7.32 (d, J = 8.0 Hz, 6H), 7.20 (t, J = 8.0 Hz, 6H), 7.13 (t, J = 7.0 Hz, 3H), 6.55 (d, J = 8.0 Hz, 1H), 6.40 (d, J = 8.0 Hz, 1H), 5.62 (m, 1H), 5.49 (d, J = 9.5 Hz,

DOI: 10.1021/acs.bioconjchem.5b00085
Bioconjugate Chem. 2015, 26, 1041–1053

1H), 4.45 (s, 1H), 4.22 (d, J = 5.5 Hz, 1H), 3.28 (s, 1H), 2.92 (d, J = 18.5 Hz, 2H), 2.56 (d, J = 8.0 Hz, 1H), 2.44 (s, 3H), 2.35 (m, 4H), 2.12 (m, 2H), 1.92 (m, 1H), 1.70 (d, J = 12.5 Hz, 1H). ^{13}C NMR (125 MHz, $CDCl_3$+CD_3OD): δ = 171.9, 144.6 (3), 144.4, 139.1, 129.5 (6), 128.7, 128.5, 127.93, 127.87 (6), 127.7, 126.7 (3), 119.4, 117.3, 92.7, 66.7, 59.4, 49.7, 47.3, 43.4, 42.5, 38.94, 38.89, 34.7, 27.7, 20.2. MS (ESI): m/z = 615.3 $[M + H]^+$. HRMS (ESI) m/z: $[M + H]^+$ calcd for 615.2681; found, 615.2675. Anal. Calcd for $C_{39}H_{38}N_2O_3S{\cdot}1.2H_2O$: C, 73.60; H, 6.40; N, 4.40. Found: C, 73.31; H, 6.07; N, 4.66.

Materials and Reagents. The NHS-$(PEG)_2$-maleimide cross-linker [(SM-$(PEG)_2$], 10 mL spin desalting columns (Zeba, 7K MWCO), dialysis cassettes (Slide-A-Lyzer G2, 10K MWCO), bicinchoninic acid (BCA) protein assay kit, bovine serum albumin (BSA), phosphate buffered saline (PBS, 100 mM sodium phosphate, 150 mM NaCl, pH 7.2) that were used for the coupling reactions were purchased from Pierce Protein Research/Thermo Fisher Scientific (Rockford, IL). Dulbecco's phosphate buffered saline (DPBS, 10 mM Na_2HPO_4, 1.8 mM KH_2PO_4, 2.7 mM KCl, 137 mM NaCl, pH 7.4), used for dialysis, was purchased from Quality Biological Inc. (Gaithersburg, MD). Polysulfone membrane filters (0.22 μm) were purchased from Pall Corporation (Port Washington, NY). The 2,4,6-trinitrobenzenesulfonic acid (TNBS) was purchased from G-Biosciences (St. Louis, MO). Trifluoroacetic acid (TFA), triisopropylsilane (TIS), dimethyl sulfoxide (DMSO), 5−5′-dithiobis (2-nitrobenzoic acid) (Ellman's reagent), sodium 2-mercaptoethanesulfonate (MESNA), L-glutamic acid, sinapinic acid, UV-transparent 96 well plates, mass spectrometry grade formic acid (FA), IgG and BSA that were used as MALDI-TOF calibration standards, BSA that was used as blocking reagent for ELISA, codeine and morphine sulfate were purchased from Sigma-Aldrich (St. Louis, MO). Mass spectrometry grade water and acetonitrile (ACN) were obtained from Fisher Scientific. ZipTip (C_4 resin) was purchased from Millipore (Billerica, MA). Tetanus toxoid (TT) was purchased from Statens Serum Institut (Copenhagen, Denmark). The cross-reactive material (CRM_{197}), which is a nontoxic mutant of diphtheria toxin, was purchased from List Biologicals Laboratories, Inc. (Campbell, CA). Liposomal lipids consisting of 1,2-dimyristoyl-*sn*-glycero-3-phosphoglycerol (DMPG), 1,2-dimyristoyl-*sn*-glycero-3-phosphocholine (DMPC), monophosphoryl lipid A (PHAD) (MPLA), and cholesterol were purchased from Avanti Polar Lipids (Alabaster, AL). Heroin HCl and 6-acetylmorphine were from Lipomed Inc. (Cambridge, MA). Immulon 2HB flat ELISA plates were from Thermo Scientific (Marietta, OH). The mouse monoclonal antibodies used as standards for ELISA quantifications: anti-morphine BD1263 (Cat. No. ab26247); anti-Tetanus Toxoid HYB-278-01 (Cat. No. ab26247), and anti-diphtheria toxin HYB 123-09 (Cat. No. ab53827) were purchased from Abcam (Cambridge, MA). Peroxidase-linked sheep anti-mouse IgG (γ-chain specific) was purchased from The Binding Site (San Diego, CA). The 2,2′-Azino-di(3-ethylbenzthiazoline-6-sulfonate) (ABTS) peroxidase substrate system was purchased from KPL, Inc. (Gaithersburg, MD).

Conjugation of 1 with TT and CRM_{197} Carrier Proteins. The thiolated **1** was conjugated to the TT and CRM_{197} carrier proteins in a two-step reaction using the NHS-$(PEG)_2$-maleimide cross-linker [(SM-$(PEG)_2$]. Surface lysines of the carrier protein were first reacted with the NHS ester end of the linker to give an activated carrier protein−maleimide intermediate. The subsequent step used the Michael addition of **1** to the maleimide end of this intermediate to yield the final carrier protein-**1** conjugates used as the heroin vaccine immunogens in this study. Optimized and quantitative coupling methods as described by Torres et al.[25] were used for reproducible synthesis and characterization of **1** conjugates with varying hapten densities (Figures 2 and 3).

Conjugates with varying hapten densities were obtained by treating the TT and CRM_{197} carrier proteins with an increasing molar conjugation ratio of the (SM-$(PEG)_2$ cross-linker to the carrier protein. The TT and CRM_{197} carrier proteins were dialyzed overnight against PBS, pH 7.2. Aliquots containing 2 mg of the protein were mixed with increasing excess molar ratios (5, 25, 100, 200, 400, and 800) of the SM-$(PEG)_2$ cross-linker (250 mM stock in DMSO) and incubated for 2 h at RT. Excess linker was removed by passing the reaction mixture through two consecutive 10 mL spin desalting columns (7K MWCO). Aliquots of this purified activated carrier protein−maleimide intermediate were taken to determine the protein concentration by BCA and the maleimide content using a modified Ellman's test, as described below.

An aqueous solution of **1** was prepared as follows: the trityl-protected hapten **1** (6 mg) was deprotected by dissolving in chloroform (656 μL, 87.5%), treating with TFA (75 μL, 10%) and TIS (19 μL, 2.5%) for 1 h at RT, and concentrating the reaction mixture under high vacuum overnight. This crude residue was purified to remove the trityl side product from hapten deprotection using petroleum ether wash (500 μL, three times) followed by thin layer chromatography to confirm the complete removal of the side product. The purified hapten was solubilized in water (1 mL) with sonication and filtered through polysulfone membrane filter (0.22 μm). The amount of thiols in this purified deprotected **1** aqueous solution was measured by Ellman's assay. Briefly, an aliquot of **1** was diluted in 100 mM sodium phosphate buffer (PB), pH 8.0 (800 μL final volume), and treated with Ellman's reagent (160 μL, 10 mM in PB, pH 8.0). The absorbance of the reaction mixture was read at 412 nm and the thiol concentration was quantified from a standard calibration curve prepared by adding the Ellman's reagent to different concentrations of MESNA, a water-soluble thiol.

The **1** solution volume corresponding to a 300-fold molar excess ratio of **1** to protein−maleimide was then calculated and added dropwise to a stirring solution of the purified activated carrier protein−maleimide intermediate. Following incubation at RT for 2 h, excess **1** was removed by overnight dialysis against DPBS, pH 7.4. The final TT-**1** and CRM_{197}-**1** conjugates were membrane filtered and the protein recovery from protein−maleimide to protein-**1** (% protein yield, Figure 3) was determined by BCA assay. The hapten equivalences/density were measured by the TNBS assay and MALDI-TOF MS, as described below. In order to confirm that all attached linker-maleimides were completely quenched by the hapten, the modified Ellman's test was also performed on the final conjugates immediately after the completion of the conjugation procedure.

Measurement of the Hapten Equivalences/Density for the TT-1 and CRM_{197}-1 Conjugates. This was done by the three different methods as described by Torres et al.[25] The hapten equivalences were measured by indirect chemical methods, i.e., the modified Ellman's test and TNBS assay and were compared to the hapten densities obtained by MALDI-TOF MS (Figure 2A,B).

Modified Ellman's Test. This test measured the concentration of maleimide in the protein−maleimide intermediates

DOI: 10.1021/acs.bioconjchem.5b00085
Bioconjugate Chem. 2015, 26, 1041−1053

by reacting the intermediates with excess MESNA and subsequently back-titrating the unreacted MESNA with Ellman's reagent. The difference between the initial and final MESNA concentration corresponded to the maleimide content of the sample, which represented hapten equivalences since the maleimide group in protein−maleimide was the reaction partner for **1**. Briefly, an aliquot of the protein−maleimide was suspended in PB, pH 7.2, and reacted with excess MESNA (160 μL, 500 μM in PB, pH 8.0). The final volume and final protein concentration, [protein−maleimide], of the reaction mixture were 800 μL and 1 μM, respectively. The reaction mixture was incubated at RT for 5 min. Ellman's reagent (160 μL, 10 mM in PB, pH 8.0) was added to the reaction and absorbance was measured at 412 nm. The amount of unreacted MESNA, $[\text{MESNA}]_{\text{final}}$, was determined from the MESNA calibration curve. The initial concentration of MESNA, $[\text{MESNA}]_{\text{initial}}$, was the excess MESNA described above without the protein. The number of maleimides per protein was calculated using the expression

$$\text{number of maleimides} = \frac{([\text{MESNA}]_{\text{initial}} - [\text{MESNA}]_{\text{final}})}{[\text{protein} - \text{maleimide}]}$$

TNBS Assay. TNBS specifically reacts with primary amines on the protein surface to give a yellow-colored product that can be monitored at 420 nm. The difference in the number of free amines before and after conjugation represented hapten equivalences because the amino group reacts with the linker during the coupling process. Briefly, the free carrier protein and the protein-**1** conjugates were suspended in 0.1 M $NaHCO_3$, pH 8.0, and treated with TNBS (250 μL, 0.01% in 0.1 M $NaHCO_3$). The final volume and final protein concentration, [protein-**1**], of the reaction mixture were 500 μL and 1 μM, respectively. The reaction was incubated for 2 h at 37 °C and the absorbance was measured at 420 nm. The free amine concentration, [Amine], was calculated from the corresponding calibration curve plotted using L-glutamic acid as a standard. The number of amines per protein was calculated using the expression

$$\text{number of amines} = \frac{[\text{amine}]}{[\text{protein}-\mathbf{1}]}$$

MALDI-TOF MS. The exact mass of the protein-**1** conjugates was determined by matrix-assisted laser desorption ionization time-of-flight mass spectroscopy (MALDI-TOF MS), using the Axima MegaTOF instrument (Shimadzu Scientific Instruments, Columbia, MD). Briefly, the unconjugated TT and CRM_{197} starting protein and the TT-**1** and CRM_{197}-**1** conjugates were desalted using C_4 ZipTip. The proteins (0.5 μL) were mixed with (0.5 μL) sinapinic acid (10 mg/mL in 50:50 ACN/H_2O 0.1% FA) and spotted on a MALDI-TOF 384-well stainless plate. The instrument was calibrated against IgG (for TT) or BSA (for CRM_{197}) MALDI-TOF calibration standards. Mass spectra of the proteins were acquired by averaging 500 mass profiles in the linear mode, smoothed using Gaussian method, and mass assignments were done using threshold apex peak detection. The number of the haptens was calculated using the expression

$$\text{number of haptens} = \frac{\text{mass}_{\text{protein}-\mathbf{1}} - \text{mass}_{\text{protein}}}{\text{mass}_{\mathbf{1}-\text{linker}}}$$

The net mass addition of **1** and linker, $\text{Mass}_{\mathbf{1}\text{-linker}}$, was 682.27 g/mol.

The size and integrity of the various conjugates were also analyzed by SDS PAGE, Blue Native PAGE,and SEC (sze exclusion chromatography)-HPLC (see Supporting Information).

Vaccine Formulation and Immunization. Liposomes with MPLA, consisting of DMPC/cholesterol/DMPG in a molar ratio of 9:7.5:1, were prepared as described.[8,46] The preformed liposomes were mixed 1:1 with the protein-**1** conjugates to give a dose of 10 μg protein per vaccine dose of 0.05 mL. The final vaccine contained 50 mM phospholipid liposomes containing 20 μg MPLA/dose in DPBS, pH 7.4. Female Balb/c mice from Jackson Laboratories (Bar Harbor, ME) (6−7 weeks of age; 13 per group) were immunized intramuscularly (IM) with 0.05 mL of the vaccines at weeks 0, 3, and 6 weeks in alternate rear thighs. All animals were bled prior to the each immunization. At 9 weeks after the primary immunization, 5 mice per group were terminally bled. The remaining 8 mice per group were used for the antinociception assays at week 9 and were not bled prior to injection of heroin (1 mg/kg, subcutaneous). These 8 mice per group were kept longer to check for longevity of vaccine responses and later bled at week 14 and then rechallenged with heroin at week 15 (Figure 4). The mouse studies testing different hapten densities of **1** on TT and CRM_{197} carriers (shown in this manuscript) were performed once, but with 13 mice per group to ensure adequate statistical power. In addition, the best performing TT-**1** conjugates with high hapten densities described here were used in 4 additional followup studies (unpublished data) and have shown similar results.

ELISA and Competition ELISA. The serum antibody levels against the heroin hapten **1** were measured over time at weeks 0, 3, 6, 9, and 14 (Figures 5 and 6). **1** was coupled to BSA using the same method as described before.[8] BSA-**1** (0.1 μg BSA/0.1 mL DPBS, pH 7.4) was added to the ELISA plates and incubated at 4 °C overnight. The remainder of the ELISA was conducted as described.[8,47] Briefly, the plates were blocked with blocker (1% BSA in 20 mM Tris-0.15 M sodium chloride, pH 7.4) for 2 h. Mouse sera and the mouse anti-morphine antibody standard were serially diluted in blocker and added to the plates in triplicate. Following incubation for 2 h at RT, the plates were washed with 20 mM Tris−0.15 M sodium chloride−0.05% Tween 20. Peroxidase linked-sheep anti-mouse IgG diluted in blocker (1:1000) was added and the plates were incubated for 1 h at RT. The plates were washed and ABTS peroxidase substrate system (100 μL/well) was added. After incubation at RT for 1 h, the absorbance was read at 405 nm. Serum anti-**1** IgG concentrations were quantified by ELISA from a standard curve of murine anti-morphine monoclonal antibody BD1263 (Abcam, Cambridge, MA; Cat. No. ab26247).

The serum antibody levels against the carrier proteins were also measured at weeks 0 and 9 (Figure 6) and at week 14 (Figure S11). For TT carrier-specific ELISA, similar protocol was followed using 0.1 μg/well TT as the coating antigen and a mouse monoclonal antibody to Tetanus Toxoid, (HYB-278-01; AbCam, Cat. No. ab26247) standard curve used for quantification. For CRM_{197} carrier ELISA, 0.05 μg/well CRM_{197} was used as the coating antigen and a mouse monoclonal anti-diphtheria toxin antibody (HYB 123-09; AbCam, Cat. No. ab53827) was used as a standard for quantification.

DOI: 10.1021/acs.bioconjchem.5b00085
Bioconjugate Chem. 2015, 26, 1041−1053

Competition ELISA was used to assess the relative ability and specificity of the vaccine-induced anti-**1** antibodies to bind heroin and heroin metabolites, 6-acetylmorphine and morphine, and also a structurally similar opiate codeine. Sera from the 4−5 individual mice euthanized at week 9 were diluted in blocker to give an ELISA absorbance of approximately 1.5. Heroin HCl and morphine sulfate were dissolved in blocker. 6-Acetylmorphine and codeine were dissolved in DMSO at 10-fold higher concentration and then diluted 10-fold in blocker. The inhibitors were diluted in 10-fold increments in a 96 well plate and mixed with diluted sera to give the final inhibitor concentrations between 0 and 10^3 μM for all opiates except for heroin, which was up to 10^4 μM. After incubation for 30 min at RT, each serum−inhibitor mixture was added to ELISA plates that were coated with BSA-**1** and blocked with BSA. The ELISA was processed as described above. Normalized curves obtained from competitive ELISAs were used to calculate the 50% inhibitory concentration (IC_{50} values)[48] of these fluid-phase drugs required to inhibit the binding of anti-**1** antibodies to plate-bound BSA-**1**. IC_{50} values were calculated from normalized curves for individual mice from each group immunized with the TT-**1** (Figure S12) and CRM_{197}-**1** (Figure S13) conjugates and are shown in SI Table S7. IC_{50} values were also calculated for the mean values of these mice grouped by the competitive opiate (Figure S14) and are shown in Table 1.

Nociception Assays. At week 9 (3 weeks after the last vaccination) and later at week 15 (9 weeks after the last vaccination), 7−8 mice from each group were tested for heroin-induced spinal (tail flick, Figure 7) and supraspinal (hot plate, Figure 8) antinociceptive responses.[49] For the tail flick test, the mice were place in a restrainer and radiant heat was applied to the tail 3 cm from the tip using the tail flick analgesia meter (Harvard Apparatus, Holliston, MA). The time from the onset of the heat to the withdrawal of the tail (latency) was measured. The intensity of the radiant heat had been adjusted previously so that baseline latencies would fall between 2 and 4 s. To avoid tissue damage, the heat stimulus was discontinued after 8 s (cutoff latency). For the hot plate test, the same mice were placed in an acrylic cylinder [20 (D) × 25 (H) cm] on a hot plate analgesia meter (Harvard Apparatus, Holliston, MA) set at 58 °C and the latency to lift or lick the hind paw or jumping was recorded. The cutoff time for this assay was 30 s. The baseline responses prior to heroin injection were measured on the tail flick followed by the hot plate assay, after which the animals were injected with 1 mg/kg of heroin HCl in saline (400 μg/mL) subcutaneously between the front shoulders, and 30 min later the tail flick and hot plate responses were measured again. These latency data from both assays were converted to percent of maximal possible effect (%MPE) as follows:

$$\%\mathrm{MPE} = \frac{(\text{test time} - \text{baseline time})}{(\text{cutoff time} - \text{baseline time})} \times 100$$

Data Analysis. Computational and statistical analysis was performed using *GraphPad Prism*. All values are reported as mean ± SEM. Antibody titers were expressed as μg/mL serum, as interpolated from the corresponding standard curves of murine monoclonal antibodies using sigmoidal, 4 parameter nonlinear regression curve fit. For calculation of the IC_{50} values for various opiates, the competition ELISA data were first normalized to correct for the different absorbances of the no inhibitor samples by calculating the percent binding. The normalized competition curves were then fitted with the log(inhibitor) vs normalized response−variable slope regression to calculate the IC_{50} values. Statistical comparison between multiple groups was performed using one-way ANOVA; Kruskal−Wallis test with Dunn's correction for multiple comparisons or two-way ANOVA; Dunnett's multiple comparisons test, as applicable. Correlation analyses were performed using nonparametric Spearman's rank correlation.

■ ASSOCIATED CONTENT

Supporting Information

Spectral data (^{1}H and ^{13}C NMR spectrum) of compounds **2**, **3**, **4**, **1**, and **7**, X-ray crystallographic data for Compound **7**, MALDI-TOF MS spectra, nonreducing SDS PAGE and Blue Native PAGE gel analysis, SEC-HPLC profiles of TT-**1** and CRM_{197}-**1** conjugates and competition ELISA data for TT-**1** and CRM_{197}-**1** antibodies from individual and grouped mice. The Supporting Information is available free of charge on the ACS Publications website at DOI: 10.1021/acs.bioconjchem.5b00085.

■ AUTHOR INFORMATION

Corresponding Author

*E-mail: gmatyas@hivresearch.org. Tel: 301-319-9973. Fax: 301-319-7518.

Author Contributions

AVM conceptualized the heroin hapten **1**. AVM, FL, JFGA, KCR, and AEJ designed, synthesized, and obtained analytical and spectral data for **1** and intermediates and JRdS obtained the X-ray spectroscopic data for compound **7**. CRA, GRM, RJ, OBT, and ZB designed and interpreted the immunological concepts and experiments for the **1** vaccine conjugates that were carried out by RJ, OBT, and GRM. RJ, CRA, GRM, and AEJ wrote the paper with input from all authors.

Notes

The authors declare the following competing financial interest(s): GRM, KCR, FL, AEJ, AVM, CRA are co-inventors in a related patent application.

■ ACKNOWLEDGMENTS

This work was supported through a Cooperative Agreement Award (no. W81XWH-07-2-067) between the Henry M. Jackson Foundation for the Advancement of Military Medicine and the U.S. Army Medical Research and Materiel Command (MRMC). The work was partially supported by an Avant Garde award to GRM from the National Institute on Drug Abuse (NIH grant no. 1DP1DA034787-01). The work of FL, JFGA, AEJ, and KCR was supported by the NIH Intramural Research Programs of the National Institute on Drug Abuse and the National Institute of Alcohol Abuse and Alcoholism, NIH, DHHS. The X-ray crystallographic work was supported by NIDA through an Interagency Agreement #Y1-DA1101 with the Naval Research Laboratory (NRL). The authors thank Drs. Klaus Gawrisch and Walter Teague (Laboratory of Membrane Biochemistry and Biophysics, NIAAA), for NMR spectral data; and Noel Whittaker (Mass Spectrometry Facility, NIDDK) for mass spectral data. The authors also thank Mr. Marcus Gallon, Ms. Elaine Morrison, Ms. Courtney Tucker, and Ms. Caroline Kittinger for providing outstanding technical assistance. Research was conducted in compliance with the Animal Welfare Act and other federal statutes and regulations relating to animals and experiments involving animals and

DOI: 10.1021/acs.bioconjchem.5b00085
Bioconjugate Chem. 2015, 26, 1041−1053

adhered to principles stated in the Guide for the Care and Use of Laboratory Animals, NRC Publication, 1996 edition. The views expressed in this article are those of the authors and do not necessarily reflect the official policy of the Department of the Army, Department of Defense, or NIH, or the U.S. Government.

■ ABBREVIATIONS USED

BSA, bovine serum albumin; TT, tetanus toxoid; CRM_{197}, cross-reactive material 197 (nontoxic mutant of diphtheria toxin); TNBS, 2,4,6-trinitrobenzenesulfonic acid; BCA, bicinchoninic acid; Ellman's reagent, 5−5′-dithiobis (2-nitrobenzoic acid); MESNA, sodium 2-mercaptoethanesulfonate; MALDI-TOF MS, matrix-assisted laser desorption ionization time-of-flight mass spectroscopy; $(SM\text{-}(PEG)_2$, $NHS\text{-}(PEG)_2$-maleimide cross-linker; %MPE, percent of maximal possible effect; DMPG, 1,2-dimyristoyl-*sn*-glycero-3-phosphoglycerol; DMPC, 1,2-dimyristoyl-*sn*-glycero-3-phosphocholine; MPLA, monophosphoryl lipid A; L(MPLA), liposomes containing monophosphoryl lipid A; ABTS, 2,2′-azino-di(3-ethylbenzthiazoline-6-sulfonate; TFA, trifluoroacetic acid; TIS, triisopropylsilane; DMSO, dimethyl sulfoxide; ACN, acetonitrile; FA, formic acid

■ REFERENCES

(1) Alving, C. R., Matyas, G. R., Torres, O., Jalah, R., and Beck, Z. (2014) Adjuvants for vaccines to drugs of abuse and addiction. *Vaccine 32*, 5382−5389.

(2) Kinsey, B. (2014) Vaccines against drugs of abuse: where are we now? *Ther. Adv. Vaccines 2*, 106−117.

(3) Kosten, T. R., and Domingo, C. B. (2013) Can you vaccinate against substance abuse? *Expert Opin. Biol. Ther. 13*, 1093−1097.

(4) Janda, K. D., and Treweek, J. B. (2012) Vaccines targeting drugs of abuse: is the glass half-empty or half-full? *Nat. Rev. Immunol. 12*, 67−72.

(5) Shen, X. Y., Orson, F. M., and Kosten, T. R. (2012) Vaccines against drug abuse. *Clin. Pharmacol. Ther. 91*, 60−70.

(6) Kinsey, B. M., Jackson, D. C., and Orson, F. M. (2009) Anti-drug vaccines to treat substance abuse. *Immunol. Cell Biol. 87*, 309−314.

(7) Orson, F. M., Kinsey, B. M., Singh, R. A., Wu, Y., Gardner, T., and Kosten, T. R. (2008) Substance abuse vaccines. *Ann. N.Y. Acad. Sci. 1141*, 257−269.

(8) Matyas, G. R., Rice, K. C., Cheng, K., Li, F., Antoline, J. F., Iyer, M. R., Jacobson, A. E., Mayorov, A. V., Beck, Z., Torres, O. B., et al. (2014) Facial recognition of heroin vaccine opiates: type 1 cross-reactivities of antibodies induced by hydrolytically stable haptenic surrogates of heroin, 6-acetylmorphine, and morphine. *Vaccine 32*, 1473−1479.

(9) Schlosburg, J. E., Vendruscolo, L. F., Bremer, P. T., Lockner, J. W., Wade, C. L., Nunes, A. A., Stowe, G. N., Edwards, S., Janda, K. D., and Koob, G. F. (2013) Dynamic vaccine blocks relapse to compulsive intake of heroin. *Proc. Natl. Acad. Sci. U. S. A. 110*, 9036−9341.

(10) Pryde, D. C., Jones, L. H., Gervais, D. P., Stead, D. R., Blakemore, D. C., Selby, M. D., Brown, A. D., Coe, J. W., Badland, M., Beal, D. M., et al. (2013) Selection of a novel anti-nicotine vaccine: influence of antigen design on antibody function in mice. *PLoS One 8*, e76557.

(11) Knuf, M., Kowalzik, F., and Kieninger, D. (2011) Comparative effects of carrier proteins on vaccine-induced immune response. *Vaccine 29*, 4881−4890.

(12) Borrow, R., Dagan, R., Zepp, F., Hallander, H., and Poolman, J. (2011) Glycoconjugate vaccines and immune interactions, and implications for vaccination schedules. *Expert Rev. Vaccines 10*, 1621−1631.

(13) Pravetoni, M., Vervacke, J. S., Distefano, M. D., Tucker, A. M., Laudenbach, M., and Pentel, P. R. (2014) Effect of currently approved carriers and adjuvants on the pre-clinical efficacy of a conjugate vaccine against oxycodone in mice and rats. *PLoS One 9*, e96547.

(14) Stephanopoulos, N., and Francis, M. B. (2011) Choosing an effective protein bioconjugation strategy. *Nat. Chem. Biol. 7*, 876−884.

(15) Hermanson, G. T. (2008) *Bioconjugation Techniques*, 2nd ed., Elsevier Inc., San Diego, CA.

(16) Lemus, R., and Karol, M. H. (2008) Conjugation of haptens. *Methods Mol. Med. 138*, 167−182.

(17) Carroll, F. I., Blough, B. E., Pidaparthi, R. R., Abraham, P., Gong, P. K., Deng, L., Huang, X., Gunnell, M., Lay, J. O., Jr., Peterson, E. C., et al. (2011) Synthesis of mercapto-(+)-methamphetamine haptens and their use for obtaining improved epitope density on (+)-methamphetamine conjugate vaccines. *J. Med. Chem. 54*, 5221−5228.

(18) Bizzini, B., Blass, J., Turpin, A., and Raynaud, M. (1970) Chemical characterization of tetanus toxin and toxoid. Amino acid composition, number of SH and S-S groups and N-terminal amino acid. *Eur. J. Biochem. 17*, 100−105.

(19) Thaysen-Andersen, M., Jorgensen, S. B., Wilhelmsen, E. S., Petersen, J. W., and Hojrup, P. (2007) Investigation of the detoxification mechanism of formaldehyde-treated tetanus toxin. *Vaccine 25*, 2213−2227.

(20) Broker, M., Costantino, P., DeTora, L., McIntosh, E. D., and Rappuoli, R. (2011) Biochemical and biological characteristics of cross-reacting material 197 CRM_{197}, a non-toxic mutant of diphtheria toxin: use as a conjugation protein in vaccines and other potential clinical applications. *Biologicals 39*, 195−204.

(21) Malito, E., Bursulaya, B., Chen, C., Lo Surdo, P., Picchianti, M., Balducci, E., Biancucci, M., Brock, A., Berti, F., Bottomley, M. J., et al. (2012) Structural basis for lack of toxicity of the diphtheria toxin mutant CRM197. *Proc. Natl. Acad. Sci. U.S.A. 109*, 5229−5234.

(22) Hutchinson, I., Archer, S., Hill, K. P., and Bidlack, J. M. (1996) Synthesis and opioid binding properties of 2-chloroacrylamido derivatives of 7,8-dihydromorphinans. *Bioorg. Med. Chem. Lett. 6*, 1563−1566.

(23) MacDougall, J. M., Zhang, X.-D., Polgar, W. E., Khroyan, T. V., Toll, L., and Cashman, J. R. (2004) Synthesis and biological evaluation of some 6-arylamidomorphines as analogues of morphine-6-glucuronide. *Bioorg. Med. Chem. 12*, 5983−5990.

(24) Welsh, L. H. (1954) O3-Monoacetylmorphine. *J. Org. Chem. 19*, 1409−1415.

(25) Torres, O. B., Jalah, R., Rice, K. C., Li, F., Antoline, J. F., Iyer, M. R., Jacobson, A. E., Boutaghou, M. N., Alving, C. R., and Matyas, G. R. (2014) Characterization and optimization of heroin hapten-BSA conjugates: method development for the synthesis of reproducible hapten-based vaccines. *Anal. Bioanal. Chem. 406*, 5927−5937.

(26) Singh, K. V., Kaur, J., Varshney, G. C., Raje, M., and Suri, C. R. (2004) Synthesis and characterization of hapten-protein conjugates for antibody production against small molecules. *Bioconjugate Chem. 15*, 168−173.

(27) Hu, K., Huang, X., Jiang, Y., Qiu, J., Fang, W., and Yang, X. (2012) Influence of hapten density on immunogenicity for anti-ciprofloxacin antibody production in mice. *Biosci. Trends 6*, 52−56.

(28) Stave, J. W., and Lindpaintner, K. (2013) Antibody and antigen contact residues define epitope and paratope size and structure. *J. Immunol. 191*, 1428−1435.

(29) Matyas, G. R., Mayorov, A. V., Rice, K. C., Jacobson, A. E., Cheng, K., Iyer, M. R., Li, F., Beck, Z., Janda, K. D., and Alving, C. R. (2013) Liposomes containing monophosphoryl lipid A: A potent adjuvant system for inducing antibodies to heroin hapten analogs. *Vaccine 31*, 2804−2810.

(30) Bonese, K. F., Wainer, B. H., Fitch, F. W., Rothberg, R. M., and Schuster, C. R. (1974) Changes in heroin self-administration by a rhesus monkey after morphine immunisation. *Nature 252*, 708−710.

(31) Akbarzadeh, A., Mehraby, M., Zarbakhsh, M., and Farzaneh, H. (1999) Design and synthesis of a morphine-6-succinyl-bovine serum albumin hapten for vaccine development. *Biotechnol. Appl. Biochem. 30* (Pt 2), 139−146.

DOI: 10.1021/acs.bioconjchem.5b00085
Bioconjugate Chem. 2015, 26, 1041−1053

(32) Anton, B., and Leff, P. (2006) A novel bivalent morphine/heroin vaccine that prevents relapse to heroin addiction in rodents. *Vaccine 24*, 3232−3240.
(33) Li, Q. Q., Luo, Y. X., Sun, C. Y., Xue, Y. X., Zhu, W. L., Shi, H. S., Zhai, H. F., Shi, J., and Lu, L. (2011) A morphine/heroin vaccine with new hapten design attenuates behavioral effects in rats. *J. Neurochem. 119*, 1271−1281.
(34) Raleigh, M. D., Pravetoni, M., Harris, A. C., Birnbaum, A. K., and Pentel, P. R. (2013) Selective effects of a morphine conjugate vaccine on heroin and metabolite distribution and heroin-induced behaviors in rats. *J. Pharmacol. Exp. Ther. 344*, 397−406.
(35) Pravetoni, M., Raleigh, M. D., Le Naour, M., Tucker, A. M., Harmon, T. M., Jones, J. M., Birnbaum, A. K., Portoghese, P. S., and Pentel, P. R. (2012) Co-administration of morphine and oxycodone vaccines reduces the distribution of 6-monoacetylmorphine and oxycodone to brain in rats. *Vaccine 30*, 4617−4624.
(36) Chen, F., Nielsen, S., and Zenobi, R. (2013) Understanding chemical reactivity for homo- and heterobifunctional protein cross-linking agents. *J. Mass Spectrom. 48*, 807−812.
(37) Metz, B., Kersten, G. F., Hoogerhout, P., Brugghe, H. F., Timmermans, H. A., de Jong, A., Meiring, H., ten Hove, J., Hennink, W. E., Crommelin, D. J., et al. (2004) Identification of formaldehyde-induced modifications in proteins: reactions with model peptides. *J. Biol. Chem. 279*, 6235−6243.
(38) Bogen, I. L., Boix, F., Nerem, E., Morland, J., and Andersen, J. M. (2014) A monoclonal antibody specific for 6-monoacetylmorphine reduces acute heroin effects in mice. *J. Pharmacol. Exp. Therapeutics 349*, 568−576.
(39) Stowe, G. N., Vendruscolo, L. F., Edwards, S., Schlosburg, J. E., Misra, K. K., Schulteis, G., Mayorov, A. V., Zakhari, J. S., Koob, G. F., and Janda, K. D. (2011) A vaccine strategy that induces protective immunity against heroin. *J. Med. Chem. 54*, 5195−5204.
(40) Pollabauer, E. M., Petermann, R., and Ehrlich, H. J. (2009) The influence of carrier protein on the immunogenicity of simultaneously administered conjugate vaccines in infants. *Vaccine 27*, 1674−1679.
(41) Dagan, R., Poolman, J., and Siegrist, C. A. (2010) Glycoconjugate vaccines and immune interference: A review. *Vaccine 28*, 5513−5523.
(42) Pobre, K., Tashani, M., Ridda, I., Rashid, H., Wong, M., and Booy, R. (2014) Carrier priming or suppression: understanding carrier priming enhancement of anti-polysaccharide antibody response to conjugate vaccines. *Vaccine 32*, 1423−1430.
(43) Pichichero, M. E. (2013) Protein carriers of conjugate vaccines: characteristics, development, and clinical trials. *Hum. Vaccines Immunother. 9*, 2505−2523.
(44) Shinefield, H. R. (2010) Overview of the development and current use of CRM(197) conjugate vaccines for pediatric use. *Vaccine 28*, 4335−4339.
(45) Simon, C., Hosztafi, S., and Makleit, S. N. (1992) Application of the Mitsunobu reaction for morphine compounds. Preparation of 6β-aminomorphine and codeine derivatives. *Synth. Commun. 22*, 913−921.
(46) Matyas, G. R., Muderhwa, J. M., and Alving, C. R. (2003) Oil-in-water liposomal emulsions for vaccine delivery. *Methods Enzymol. 373*, 34−50.
(47) Li, F., Cheng, K., Antoline, J. F., Iyer, M. R., Matyas, G. R., Torres, O. B., Jalah, R., Beck, Z., Alving, C. R., Parrish, D. A., et al. (2014) Synthesis and immunological effects of heroin vaccines. *Org. Biomol. Chem. 12*, 7211−7232.
(48) Zhang, H., Wang, S., and Fang, G. (2011) Applications and recent developments of multi-analyte simultaneous analysis by enzyme-linked immunosorbent assays. *J. Immunol. Methods 368*, 1−23.
(49) Bannon, A. W., and Malmberg, A. B. (2007) Models of nociception: hot-plate, tail-flick, and formalin tests in rodents. *Curr. Protoc. Neurosci.* Chapter 8, Unit 8 9.

DOI: 10.1021/acs.bioconjchem.5b00085
Bioconjugate Chem. 2015, 26, 1041−1053